

# Supplemental Material: Imaging pinning and expulsion of individual superconducting vortices in amorphous MoSi thin films

L. Ceccarelli, D. Vasyukov, M. Wyss, G. Romagnoli, N. Rossi, L. Moser, and M. Poggio

Department of Physics, University of Basel, 4056 Basel, Switzerland

## I. SQUID-on-tip characteristics

The SQUID-on-tip (SOT) sensor used here is made by evaporating Pb on the apex of a pulled quartz capillary according to a self-aligned method described in Vasyukov et al [1]. A typical SOT is shown in the scanning electron micrographs (SEMs) of Fig. S1. The two evaporated Pb leads are visibly separated by an insulating gap. The zoomed-in SEM shows the size of the SQUID loop at the tip.

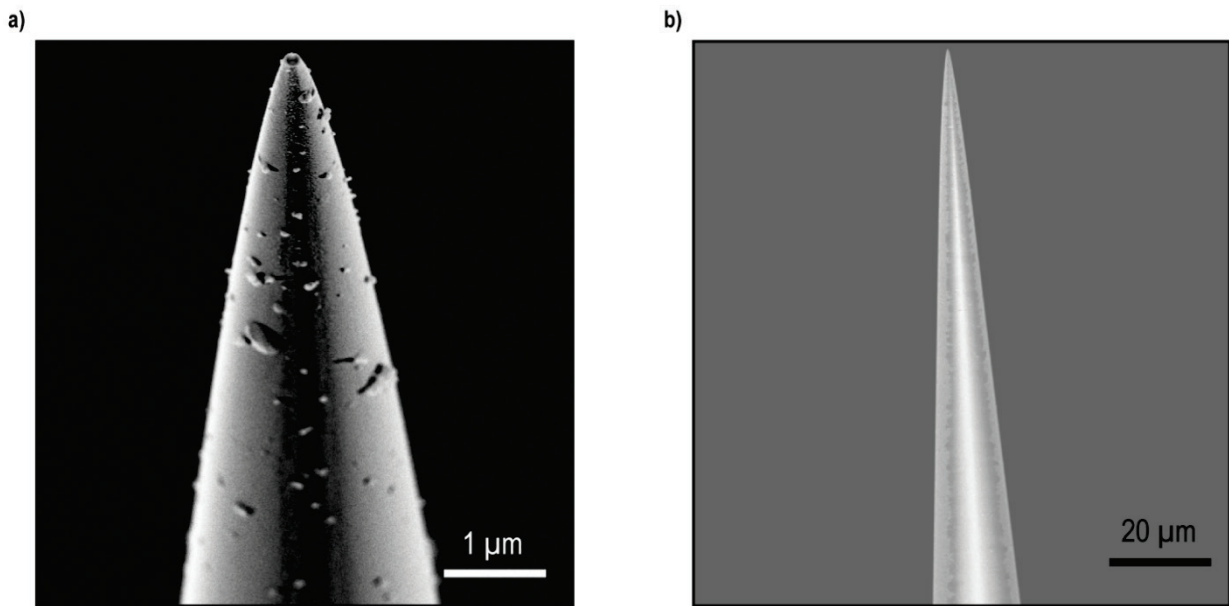
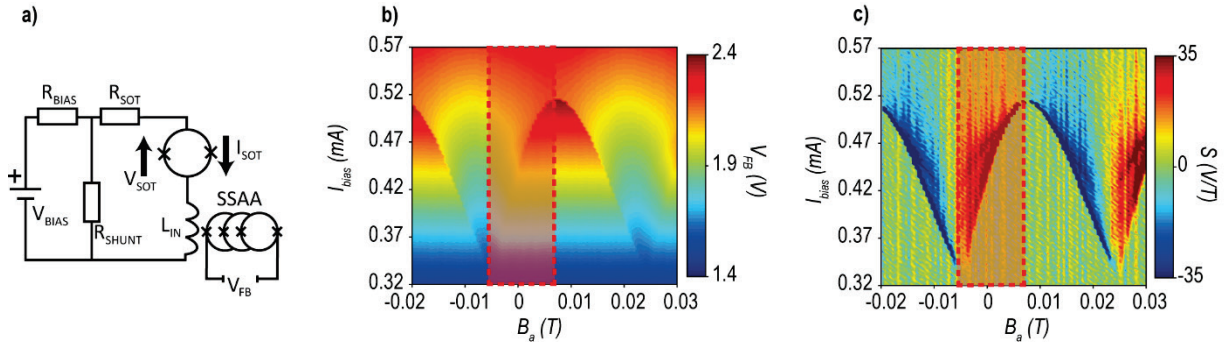


Figure S1: SEMs of a typical SOT sensor. a) zoomed-in and b) zoomed-out views.

The effective diameter of this SQUID loop can be determined from the quantum interference pattern measured at  $T = 4.2$  K using the circuit shown in Fig. S2 (a). The SOT shows pronounced critical current  $I_c(B_o)$  oscillations, shown in Fig. S2 (b) with a period corresponding to an effective loop diameter of 310 nm. A serial SQUID array amplifier (SSAA) is used to measure the current passing through the SOT  $I_{SOT}$  yielding an output voltage  $V_{FB}$  proportional to  $I_{SOT}$ . The sensitivity of the SOT to magnetic field for

various  $I_{bias}$  and  $B_a$  is shown in Fig. S2 (c) by plotting  $\frac{\partial V_{FB}}{\partial B_a}$ . This map is used to determine its sensitivity to magnetic field. Note that for certain values of  $B_a$ , the SOT is nearly insensitive to variations in magnetic field.

It is interesting to observe that the SQUID interference pattern of this particular device is not symmetric respect to  $B_a = 0$  T. This shift of the pattern is due to the asymmetry of the two Dayem bridge junctions. In our case, this asymmetry was produced intentionally by modifying the fabrication recipe, so that we could investigate the vortex state of the MoSi sample even for very small  $B_a$ .



**Figure S2: SOT circuit and quantum interference.** a) SOT measurement circuit diagram. b) Quantum interference of the SOT and b) its derivative with respect to  $B_o$ .

## II. Sample thickness, surface, and composition

The thickness of the MoSi film is an important parameter, which determines whether our system resides in the superconducting thin-film limit and what kind model should be used to describe the penetrating magnetic flux. The thickness was measured both by atomic force microscopy (AFM) and SEM. Figs. S3 a) and b) show SEM and AFM measurements of the same area, showing the edge of a MoSi wire and the transition from etched SiO<sub>2</sub> to the MoSi thin-film. An AFM line-cut, taken along the blue line in Fig. S3 b) is depicted in Fig. S3 c). The two dashed red lines in Fig. S3 b) and c) denote the edge of the MoSi layer, whose thickness is highlighted in green in Fig. S3 c).

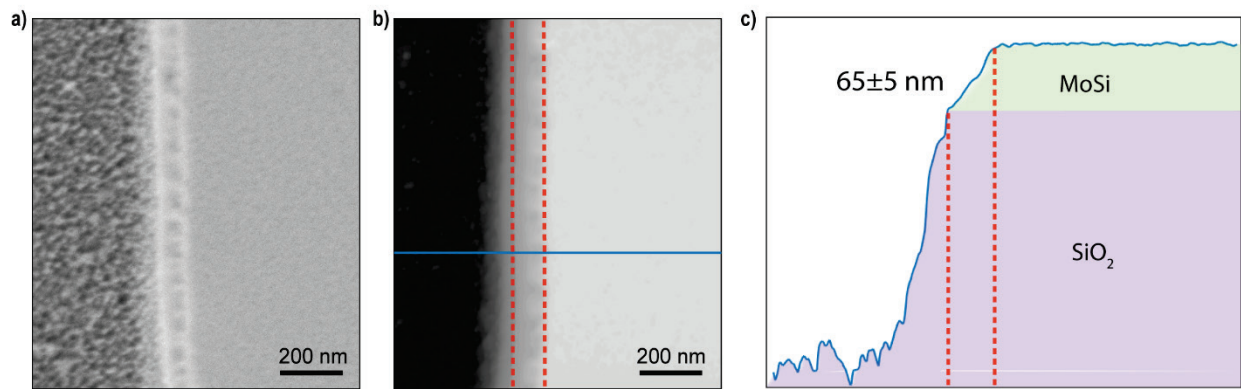


**Figure S3: SEM and AFM of MoSi sample.** a) SEM of an edge of the MoSi wire. The dark region is  $\text{SiO}_2$  and the light region is the MoSi. b) AFM image of the same region with dark contrast corresponding to low parts of the sample and light contrast to high parts of the sample. c) Line cut of the AFM in b).

Structural and surface defects in the MoSi film are shown in Figs. S4 a) and b) as inclusions and roughness on the surface. These defects are especially prominent near the edges of the sample. Wide-field SEM of the MoSi sample is shown in Fig. S5 a). The red-square highlights the area corresponding to the SEM and magnetic map reported in Figs. 1 b) and c), in the main text.

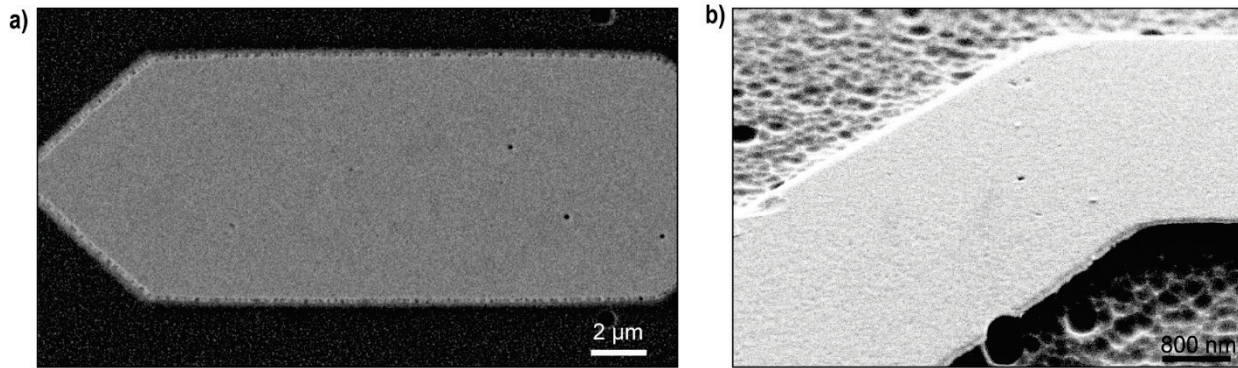


Figure S4: SEMs of MoSi sample from the a) top and from b) an oblique angle.

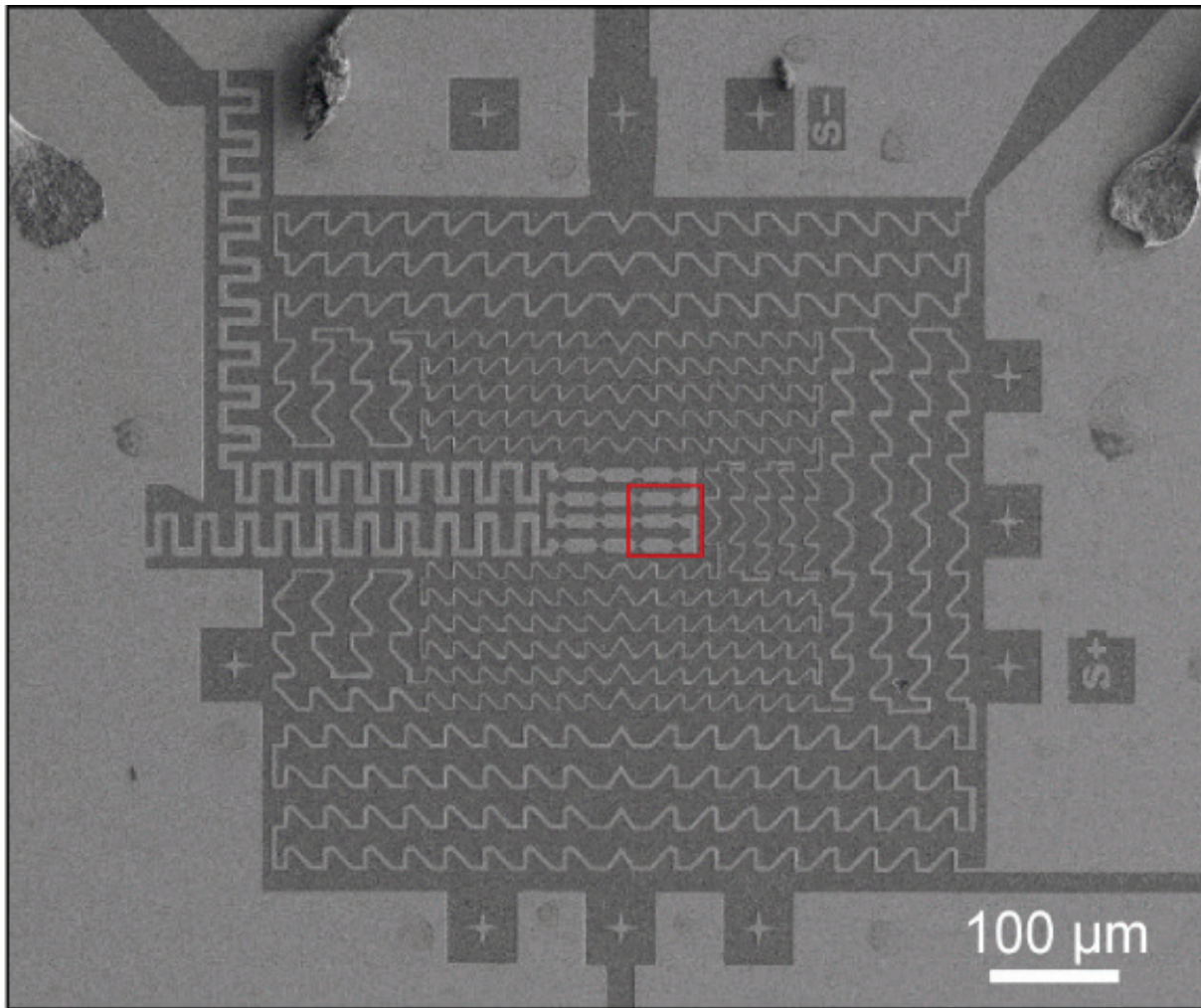


Figure S5: Wide-field SEM of the MoSi sample.

In order to confirm the high purity of the Mo-Si wafers, we perform X-ray photoelectron spectroscopy (XPS) characterization of MoSi film used to produce the wire samples (figure S8). Besides the two elements constituting the samples (Mo and Si), only oxygen and carbon are measured. Their presence is due to atmosphere contamination as the samples are exposed to air during the process. Two fine scans of the Mo3d and Si2p regions are done to identify the different chemical states and are fitted to provide the most accurate composition calculations as possible. Both Mo and Si are found in a MoSi alloy state (227.6 and 99 eV, respectively) and oxide state (232.2 and 102 eV, respectively), where the latter is expected due to air exposure [2]. In terms of elemental composition, the surface is composed of 24 at. % of Si for 76 at. % of Mo.

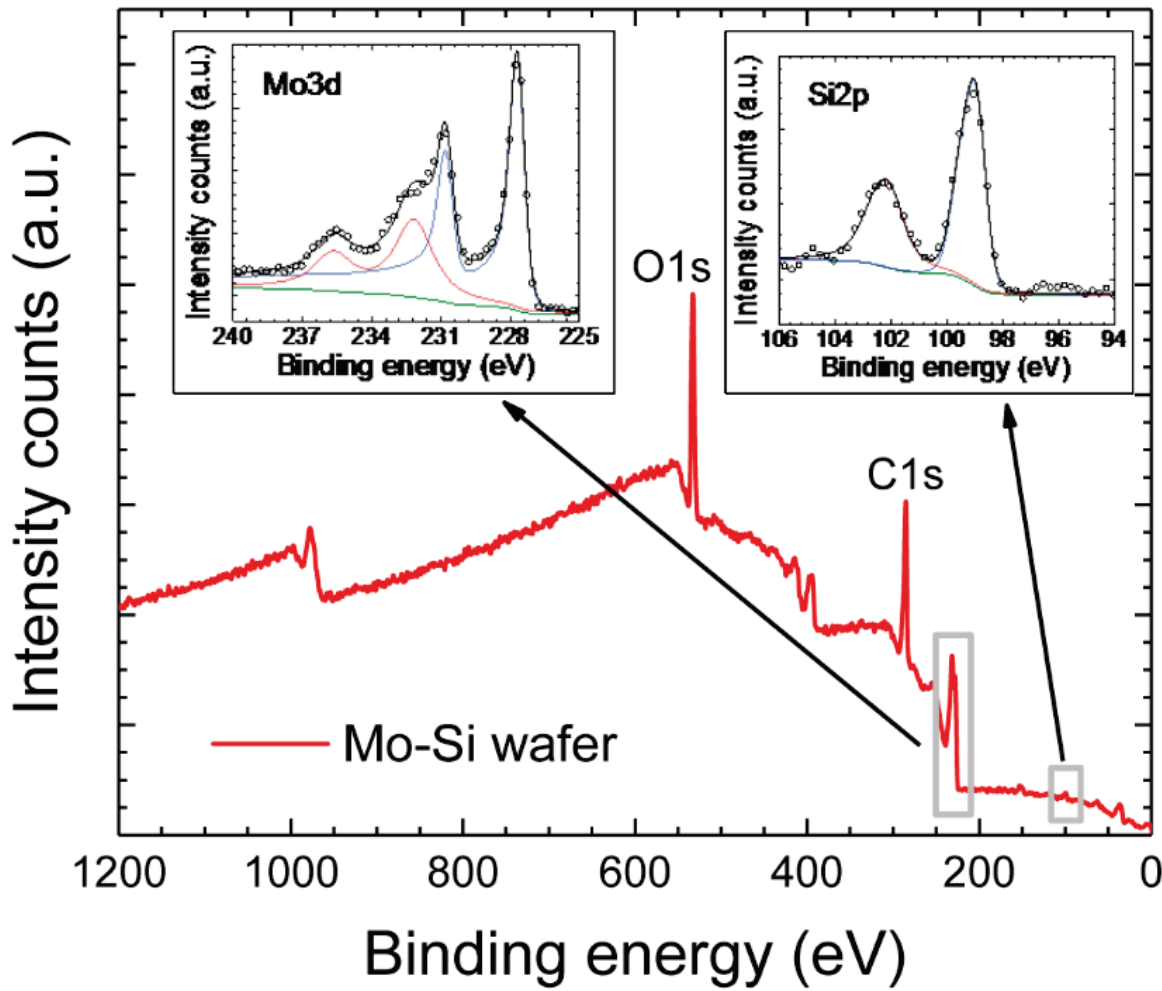


Figure S8: XPS characterization of the MoSi film shown in red. Two narrow scans of the Mo3d and Si2p regions are shown as insets. The shown spectra are normalized for comparison. The open circles are the measured data and the black lines correspond to the sum curve of all components represented in colored lines.

## References

- [1] D. Vasyukov, Y. Anahory, L. Embon, D. Halbertal, J. Cuppens, L. Neeman, A. Finkler, Y. Segev, Y. Myasoedov, M. L. Rappaport, M. E. Huber, and E. Zeldov, *Nat Nano* **8**, 639 (2013).
- [2] R. Gago, M. Jaafar, and F. J. Palomares, *J. Phys.: Condens. Matter* **30**, 264003 (2018).